Identification of contact angle and heterogenity detection in tactile images

Dmitriy E. Alexandrov and Stepan A. Nersisyan

***Abstract*—*Introduction*.** Automated analysis of tactile images registered by specialized medical tools is a novel domain, which results promptly find their applications in clinical practice. Medical Tactile Endosurgical Complex (MTEC) is currently the only commercially available device for intraoperative instrumental mechanoreceptoric palpation. One of the main challenges related to processing data generated by MTEC is heterogeneity detection in tactile images. This problem is highly important because it is a key step of localization of visually undetectable pathologies using instrumental palpation.

Objectives. One of the main difficulties related to the problem of heterogeneity detection is a possibility to vary contact angle between mechanoreceptor and sample during tactile examination, so the aim of the research was to develop a method for automated contact angle identification and detection of heterogeneity in tactile images registered by MTEC.

Methods. The proposed method of a tactile press contact angle estimation is based on classification with a specifically designed feature space. For heterogeneity detection we developed two different approaches. The first one is based on separation of heterogeneity detector into several components corresponding to similar contact angles. The second approach uses standard classification approach with contact angle as a high weighted element of the feature space.

Results. Validation on a set of samples modeling normal tissues and pathologies showed high accuracy for contact angle identification. Both methods of heterogenity detection provided approximately the same accuracy clearly outperforming previously available methods in case of significant deviations of a contact angle from zero.

Conclusion. The methods developed provide an accurat solution for problems of contact angle identification and detection of heterogeneity even in case of significant contact angle deviations, and such deviations are unavoidable in clinical practice, especially in minimally-invasive surgery.

***Keywords*—**Medical Tactile Endosurgical Complex, tactile image, k-nearest neighbors, support vector machine.

I. Introduction

TACTILE feedback is extensively used in open surgeries to detect pathological tissues via palpation. However in case of laparoscopic or thoracoscopic operations surgeons do not have direct access to operated tissues, so conventional manual palpation becomes inapplicable. Other methods used for localization of visually undetectable pathologies, such as preoperative tattooing, ultrasound examination, etc. do not provide 100% localization rate ([1], [2]).

The research was supported by the Russian Science Foundation (project 16-11-00058 "The development of methods and algorithms for automated analysis of medical tactile information and classification of tactile images").

D. E. Alexandrov is with the Faculty of Mechanics and Mathematics, Lomonosov Moscow State University, Leninskie Gory 1, Moscow 119991, Russia (e-mail: dalexandrov@intsys.msu.ru).

S. A. Nersisyan is with the Faculty of Mechanics and Mathematics, Lomonosov Moscow State University, Leninskie Gory 1, Moscow 119991, Russia (phone: +7 (985) 125-23-00; fax: +7 (495) 939-20-90; e-mail: s.a.nersisyan@gmail.com).

One of possible ways to increase this rate is using a tactile mechanoreceptor that provides instrumental mechanoreceptoric palpation. A number of devices for instrumental tactile diagnostics are available [3], [4], [5], but to the best of our knowledge the only commercially available device for intraoperative instrumental mechanoreceptoric palpation is the Medical Tactile Endosurgical Complex (MTEC) [6], [7]. A key component of MTEC is a tactile mechanoreceptor, which pressure sensors perform registration of tactile images. In a certain sense a tactile mechanoreceptor plays the role of a finger that is used for instrumental palpation in endoscopic surgeries, including robot-assisted ones ([7], [8], [9]).

Currently surgeons mainly rely on visual or tactile reproduction of data registered by a tactile mechanoreceptor. A suspected region is inspected to detect boundaries of a pathology. It is highly desirable to develop methods for automated analysis that indicate regions of heterogeneity (since tactile properties of pathological tissues and adjacent normal tissues are essentially different [7], [10]). However note that heterogeneity does not necessarily indicate pathology; it can be caused e.g. by a blood vessel. Hence in order to reduce false positives it makes sense to enrich a heterogeneity detector with a heterogeneity classifier so that the final decision is "homogeneity", "normal heterogeneity" or "pathological heterogeneity".

A number of simple methods for automated heterogeneity detection were proposed by Solodova *et al*. in [11]. The authors showed that these methods work well when inspected surface is orthogonal to a mechanoreceptor. However it is not always possible to achieve orthogonality, and obviously the angle between an operating head and a surface essentially affects pressure values. We tested methods from [11] against a library of artificial samples and a set of contact angles. In case of fairly significant angle deviations heterogeneity detection resulted in high error rates. Another problem is inability of these methods to distinguish between normal and pathological heterogeneities.

Nersisyan *et al*. in [12] applied k-nearest neighbors-based classification algorithm with an enriched feature space to six classes of tactile images obtained under several contact angles. Results were fairly decent, however some classes were significantly confused.

We hypothesized that evaluation of a contact angle could essentially increase the quality of heterogeneity detection. One of possible strategies is to split a training set into groups corresponding to similar contact angles, to train separate classifiers for every group, to estimate the angle of an image being classified and to apply the classifier corresponding to

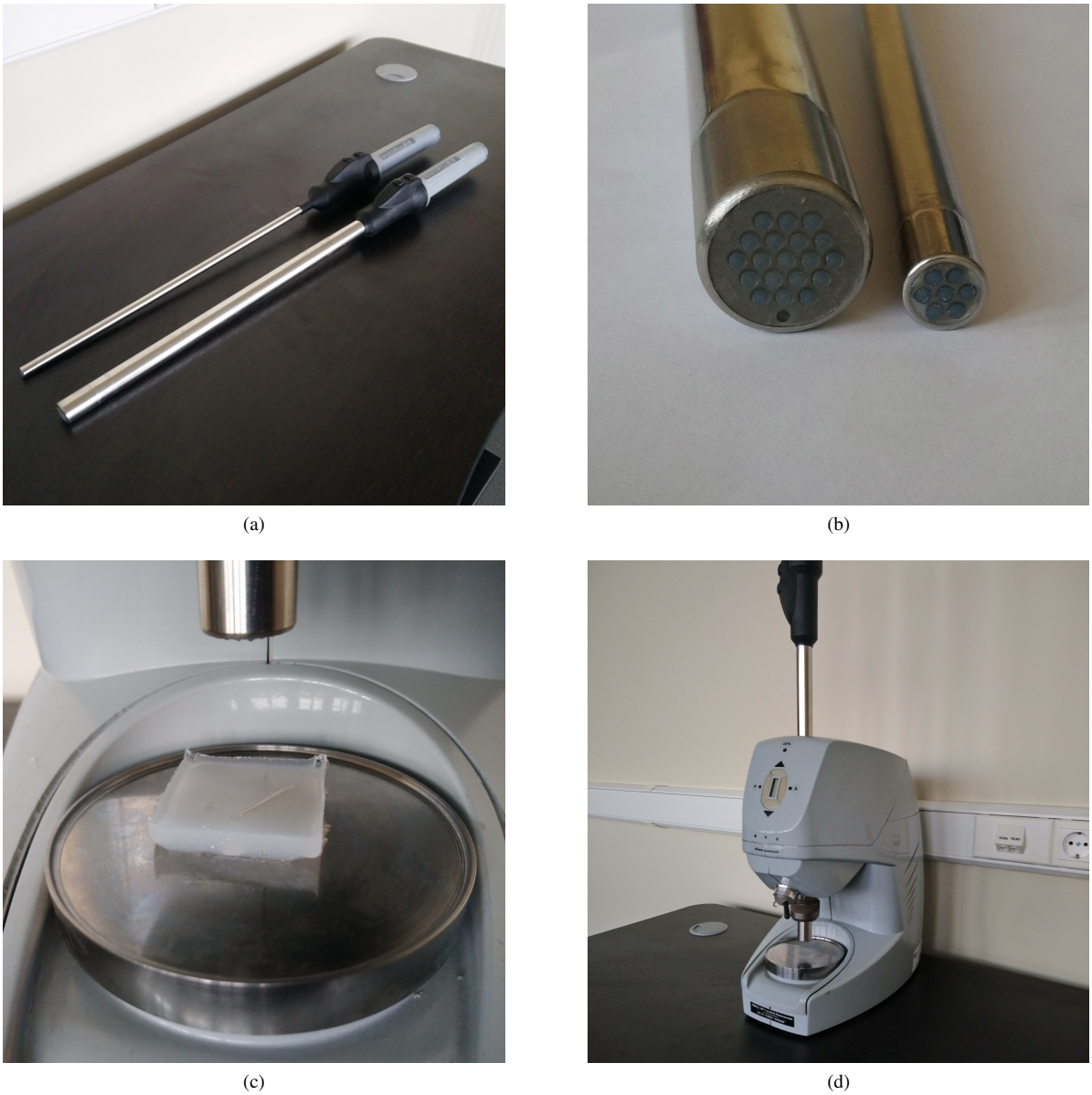

(a) (b)

(c) (d)

Fig. 1: Medical Tactile Endosurgical Complex. (**a**) Tactile mechanoreceptors. (**b**) Operating head of tactile mechanoreceptors. The left device contains 19 pressure sensors, and the right one contains 7 sensors. (**c**) A soft silicon sample imitating tissue with a blood vessel. (**d**) Experimental device allowing to perform automated sample inspection under different angles.

the angle estimated. Another strategy is to add the angle estimation as one of the features that has a large weight. We tested these strategies against a set of artificial samples modeling normal tissues, tissues with blood vessels ("normal" heterogeneity) and tissues with pathologies of sereral types and forms ("abnormal" heterogeneity). It turned out that both angle detection and classification provide high accuracy.

The rest of the paper is organized as follows. Section II gives an overview of a tactile mechanoreceptor, and section III describes the experiment setup. Section IV is devoted to verification of methods from [11]. In section V we present and validate a method for contact angle estimation. Section VI is focused on classification with known contact angles. Finally, section VII is a conclusion.

II. Tactile Mechanoreceptor

To the best of our knowledge, tactile mechanoreceptor is the only commercially available medical device for intraoperative registration of tactile images. It consists of an operating head (its diameter is either 10 mm or 20 mm) containing pressure sensors (7 or 19), and a handle (Fig. 1a, 1b). Pressure sensors form a hexagonal lattice. Pressure values are integers from the range [0; 255]. Sensors wirelessly transmit their values to a computer 100 times per second. A surgeon can press an operating head against a tissue of interest, record a sequence of pressure values and then lift the operating head back. From the formal point of view such press (called a tactile image) consists of a sequence of tactile frames $F_1, \ldots, F_n$ $(n \in \mathbb{N})$ sent by the operating head. If we enumerate pressure sensors

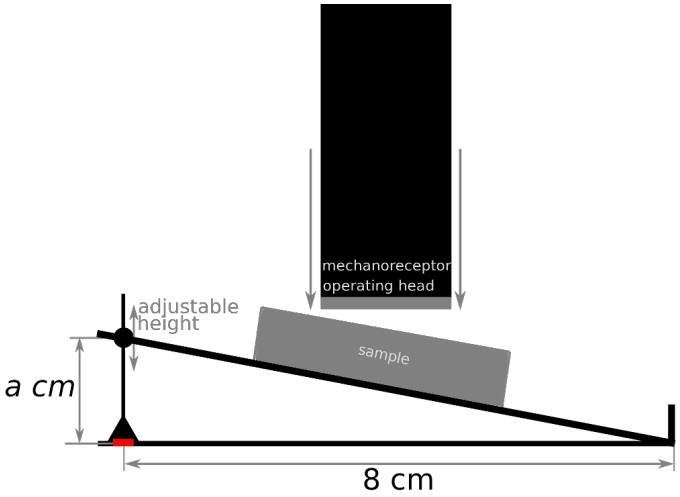

Fig. 2: A scheme of the experiment setup.

then every tactile frame is an array $s_1, \ldots, s_k$, where k is equal either to 7 or to 19. We focus on the case $k = 19$.

III. Experiment Description

For our research we manufactured samples from soft silicone (Shore hardness 00-10A) to model three different types of tissues:

1) Normal tissues: samples without any embedments;
2) Tissues with blood vessel: samples with a segment of a medical perfusion line (B. Braun Original Perfusion Line, diameter ca 2 mm) which is oriented for palpation horizontally;
3) Pathological tissues: samples with embedded spherical caps of different size (base diameter 8 mm and height 2.4 mm, or base diameter 4.7 mm and height 1.7 mm) which can be oriented for palpation from flat or convex side.

As in [12], [13], all samples had similar size: 40 mm $\times$ 35 mm $\times$ 10 mm (Fig. 1c).

Samples manufactured were examined by MTEC under five different contact angles: $0°, 3.6°, 7.1°, 10.6°$ and $14.0°$. Verticality of a press was ensured by using a device shown in Fig. 1d. The contact angle was controlled by the parameter a, see Fig. 2. As a result we obtained a collection of 450 tactile images with 90 images per angle. Types of samples were distributed across images in the following way: 75 images of normal tissues, 75 images of tissues with blood vessel and 300 images of pathological samples.

IV. Verification of Methods from [11]

We examined the performance of all methods for automated detection of heterogeneity in tactile images proposed by Solodova *et al.* in [11]. The first method is based on intraframe analysis and uses simple comparison of maximum and minimum values inside one frame. If the difference between these values exceeds a predefined threshold, a sample is classified as heterogeneous. The other two approaches use simultaneously several subsequent tactile frames. In a simpler case (the second method) an increase of pressure values in a fixed time step is computed and scaled for each sensor. Scaling pursues two goals: suppressing increase for low pressure values and integration of increase of pressure values with pressure values themself into one characteristic. Then a regularized ratio of maximum and minimum values of these characteristics is computed and compared to a predefined threshold. If this threshold is exceeded, the method reports identification of heterogeneity. The third method is similar to the second one. The difference is that increase is divided by a time step (so we get a physically meaningful speed of pressure increase), and instead of considering a fixed time step, max-min regularized ratio is additionally maximized over a segment of time steps. A detailed description of these methods can be found in [11].

We used algorithm parameters from [11]. Examination of samples with no deviation of contact angle from the zero one revealed that only the second method provided appropriate detection (sensitivity over 97%, specificity 100%), while two other methods showed unsatisfactory specificity (60% for the first method and under 10% for the third method). Furthermore, angle deviation equal to $10.6°$ reduced specificity for the second method to 60%. For deviation $14.0°$ specificity dropped further to 0%. Detailed results are presented in Table I.

These data show that examined simple methods are reliable for small deviations of a contact angle from the zero one and are generally applicable in case of medium deviations. However, for larger deviations these methods do not provide an acceptable result.

V. Contact Angle Estimation

We utilized the following strategy to estimate contact angles. The first step is preprocessing. All tactile frames that contain pressure values less than 10 or greater than 245 are discarded. Pressure values that are less than 10 normally correspond to the situation when some sensors are yet not in contact with a sample, and pressure values greater than 245 usually mean saturation of some sensors. As a result of preprocessing some tactile images were completely removed, and the remaining set consisted of 411 samples: 90 images for $0°$ and $3.6°$, 82 images for $7.1°$, 78 images for $10.6°$ and 71 for $14.0°$.

At the second step we use the least squares method to construct a linear function

$$l(x, y) = ax + by + c$$

which approximates pressure values of sensors located at operating head border (we assume that distance between sensors is equal to 1). After that we compute the angle between the planes $z = \frac{l(x,y)}{64}$ and $z = 0$. Scaling factor $\frac{1}{64}$ was selected empirically. This procedure is applied to each tactile frame that was not discarded during preprocessing.

The third step is mapping the tactile image to the feature space. We evaluate maximal, mean and median angles for the set of tactile frames of the image; these three values with all pressure values derived from the frame with the maximal angle are associated with an image as its list of features.

TABLE I: Sensitivity and specificity of simple methods for heterogeneity detection. For each case *sensitivity / specificity* are specified.

	0°	3.6°	7.1°	10.6°	14.0°
Method 1	100% / 60%	100% / 40%	100% / 0%	100% / 0%	100% / 0%
Method 2	97% / 100%	90% / 100%	95% / 100%	100% / 60%	100% / 0%
Method 3	100% / 6%	100% / 0%	100% / 0%	100% / 0%	100% / 0%

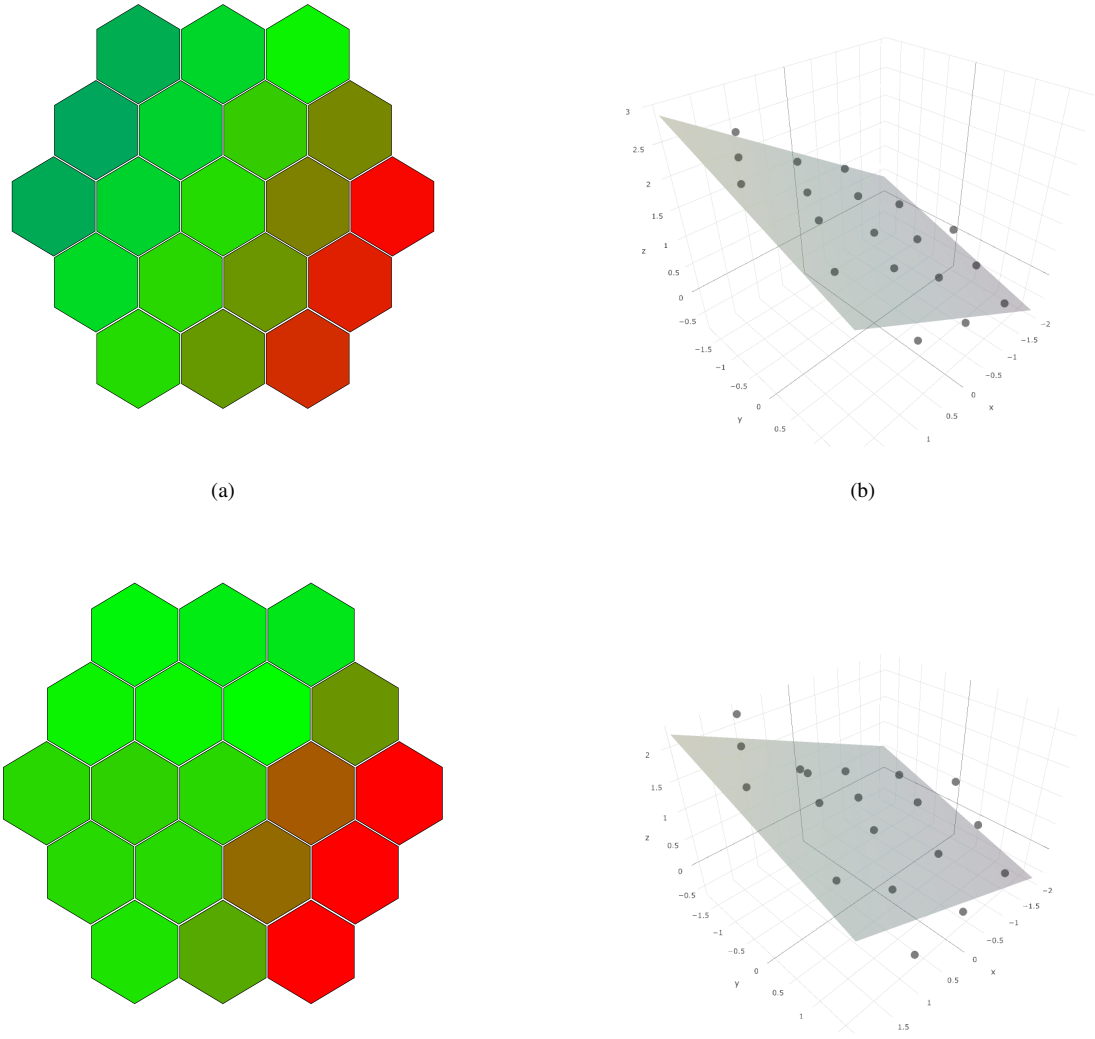

(a) (b)

(c) (d)

Fig. 3: Tactile frames and corresponding constructed planes. (**a-b**) A tactile frame and the plane derived from an examination of a sample without any embedbents under contact angle equal to $14°$. (**c-d**) A tactile frame and the plane derived from an examination of a sample with a hard embedbent imitating blood vessel under zero contact angle.

Finally, we apply a classifier to determine the angle. We utilized two different classifiers: SVM ([14]) and the k-nearest neighbor method ([15]). The following parameters were used:

- SVM: RBF kernel with parameter $\gamma = 1/22$, "one-vs-one" decision for multi-class strategy;
- k-NN: $k = 1$, the Euclidean metric.

There are two main reasons why classification step can not be avoided, i.e. why the value of the contact angle can not be computed directly. First, there is no information about sample deformation during the examination. Thus, we do not know anything about the type of dependency of angle on pressure values. The idea of direct scaling the angle between planes failed; deviation of this value even for one tactile image was quite significant. The second factor is possible presence of various embedments — high pressure value can be observed both when we examine non-homogenous tissues and when we examine homogenous tissues under non-zero angles. Fig. 3 shows tactile frames and corresponding planes for two cases:

TABLE II: Averaged confusion matrix for angle classification using SVM. Row names are labels of predicted classes, and column names are labels of true classes.

	0°	3.6°	7.1°	10.6°	14.0°
0°	69.0	18.6	3.4	1.9	1.0
3.6°	14.3	54.9	15.0	2.1	0.0
7.1°	6.5	15.9	55.5	13.7	1.3
10.6°	0.2	0.2	5.9	43.6	4.7
14.0°	0.0	0.4	2.2	16.7	64.0

TABLE III: Averaged confusion matrix for angle classification using k-NN. Row names are labels of predicted classes, and column names are labels of true classes.

	0°	3.6°	7.1°	10.6°	14.0°
0°	73.4	6.5	2.6	1.0	0.1
3.6°	9.3	72.7	9.2	3.4	0.6
7.1°	7.3	8.9	62.7	5.2	0.5
10.6°	0.0	1.9	7.5	66.2	3.9
14.0°	0.0	0.0	0.0	2.2	65.9

TABLE IV: Averaged confusion matrix for tissue type classification using the combination of five classifiers. Row names are labels of predicted classes and column names are labels of true classes.

	Normal	Pathology	Vessel
Normal	74.6	5.5	0
Pathology	0.4	293.8	2.9
Vessel	0	0.7	72.1

TABLE V: Averaged confusion matrix for tissue type classification with pressure angle value added to the feature space. Row names are labels of predicted classes and column names are labels of true classes.

	Normal	Pathology	Vessel
Normal	75.0	6.5	0
Pathology	0	293.2	4.3
Vessel	0	0.3	70.7

a sample of type 1 (no embedbments) inspected under $14°$ (Fig. 3a, 3b) and a sample of type 2 ("blood vessel") inspected under zero angle (Fig. 3c, 3d). As one can see results are visually indistinguishable.

We tested the approach proposed by applying 10 runs of 5-fold stratified cross-validation. Averaged confusion matrices for both classifiers are in Tables II and III. The results showed that classification quality was acceptable for both classifiers. Note that in both cases the major part of errors correspond to classes that are "neighbors" of the true one. However, accuracy of the nearest neighbor classifier was higher than for the SVM classifier.

VI. Tissue Type Classification

For highlighting importance of knowledge of contact angle we performed some experiments with supervised pattern recognition. Namely, we worked on the problem of tissue type identification (normal, vessel, pathology). Two approaches to classification were tested.

The idea of the first approach is to split the classifier into several components corresponding to similar contact angles. This idea was implemented in the following way. For each of the 5 given pressure angles we construct a separate classifier using the approach from [12]. For a new unclassified sample we first decide contact angle and then use the appropriate classifier.

The second approach is based on considering the contact angle returned by the angle detection procedure as an additional feature in the classifier from [12]. In order to highlight the importance of contact angle we use a large weight value for this feature.

Speaking in more detail, for the case of the first approach the feature set consists of 19 pressure values and 38 partial derivatives derived from the frame with maximal pressure variance and 4 largest values from the list of standart deviations computed for each of 19 sensors in whole tactile image. All features have the weight equal to 1. In the second case we additionally consider the contact angle with the weight ω equal to 100 (this value was selected empirically). In both cases we use the one nearest neighbor algorithm with ℓ^1-like metric:

- for the first approach the feature space has dimension 19 + 38 + 4 = 61, so the distance between points $x = (x_1, \ldots, x_{61})$ and $y = (y_1, \ldots, y_{61})$ is computed as
$$\rho(x, y) = \sum_{i=1}^{61} |x_i - y_i|;$$
- for the second approach the feature space has dimension 61 + 1 = 62; suppose that the contact angle corresponds to the coordinate number 62, then the distance between points $x = (x_1, \ldots, x_{62})$ and $y = (y_1, \ldots, y_{62})$ is computed as
$$\rho(x, y) = \sum_{i=1}^{61} |x_i - y_i| + \omega |x_{62} - y_{62}|,$$
$\omega = 100$.

To model this scheme and measure the quality of recognition we performed 10 runs of 5-fold stratified cross-validation for each angle and then averaged confusion matrices by all cross-validation runs and all angles. The final confusion matrix for the first approach is presented in Table IV. Total classification accuracy (i.e. ratio of correct predictions and the total number of samples) was equal to 97.8%. The final confusion matrix for the second approach is presented in Table V; total classification accuracy was equal to 97.5%.

Generally, results for two methods were almost the same, both for the case of three classes (as it is shown above) and for the case of two clasess "healthy" and "pathology" (obtained by uniting classes 1 ("normal") and 2 ("vessel")). In the latter case we see very low false negatives rates: 2.0% for the first method and 2.2% for the second method, and slightly higher false positives rates: 2.2% and 2.8%, respectively.

For further analysis and for comparison with previous approaches from Section IV we computed sensitivities and

TABLE VI: Sensitivity and specificity of the proposed methods for heterogeneity detection. For each case *sensitivity / specificity* are specified.

	0°	3.6°	7.1°	10.6°	14.0°
Combinied classifiers	99% / 94%	99% / 97%	95% / 99%	100% / 99%	96% / 98%
One classifier	98% / 95%	99% / 97%	95% / 100%	100% / 99%	96% / 97%

specificities for each contact angle, see Table VI. It can be seen that for the three smallest angle deviations 0°, 3.6° and 7.1° both proposed approaches and the best method from Section IV (Method 2) provides approximately the same accuracy in terms of sensivity and specificity. However for larger deviations we see that specificities of all methods from Section IV essentially dropped, while the methods from this section keep working.

VII. Conclusion

Automated analysis of tactile images registered by specialized medical tools is a novel domain, which results promptly find their applications in clinical practice. In this paper we proposed a method for automated contact angle identification and detection of heterogeneity in tactile images registered by the Medical Tactile Endosurgical Complex (MTEC). MTEC is currently the only commercially available device for intraoperative instrumental mechanoreceptoric palpation, and heterogeneity detection in tactile images registered by MTEC is a key step of localization of visually undetectable pathologies using instrumental palpation. We propose two methods that decide whether tissue is homonegeous, contains a normal heterogeneity or a pathological heterogeneity. Both methods consist of two stages. First we identify the contact angle of a tactile press using classification with a specifically designed feature space. Next we perform heterogeneity classification. In case of the first method we separate the classifier detector into several components corresponding to close contact angles. In case of the second method we add the angle identified to the feature space as a feature with a high weight. Validation on a set of samples modeling normal tissues and pathologies showed that our methods clearly outperform previously available methods in case of a significant deviation of a contact angle from zero, and this deviation is unavoidable in clinical practice, especially in minimally-invasive surgery. Thus, inclusion of the proposed methods to MTEC software will be the next step towards simpler and at the same time more efficient localization of visually undetectable pathologies using intraoperative mechanoreceptoric palpation.

Acknowledgment

The authors thank Dr. Alexei V. Galatenko, Dr. Vladimir V. Staroverov and Dr. Vladimir V. Galatenko for valuable comments and discussions.

References

[1] S. A. Acuna, M. Elmi, P. S. Shah, N. G. Coburn, and F. A. Quereshy, "Preoperative localization of colorectal cancer: a systematic review and metaanalysis," *Surg. Endosc.*, vol. 31, no. 6, pp. 2366–2377, Oct. 2017.

[2] I. S. Reynolds, M. H. Majeed, I. Soric, M. Whelan, J. Deasy, and D. A. McNamara, "Endoscopic tattooing to aid tumour localisation in colon cancer: the need for standardisation," *Ir. J. Med. Sci.*, vol. 186, no. 1, pp. 75–80, Sept. 2017.

[3] V. Egorov and A. P. Sarvazyan, "Mechanical imaging of the breast," *IEEE Trans. Med. Imaging*, vol. 27, no. 9, pp. 1275–1287, Sept. 2008.

[4] R. E. Weiss, V. Egorov, S. Ayrapetyan, N. Sarvazyan, and A. Sarvazyan, "Prostate mechanical imaging: a new method for prostate assessment," *Urology*, vol. 71, no. 3, pp. 425–429, Mar. 2008.

[5] H. van Raalte and V. Egorov, "Tactile Imaging Markers to Characterize Female Pelvic Floor Conditions," *Open J. Obstet. Gynecol.*, vol. 5, no. 9, pp. 505–515, Aug. 2015.

[6] V. Barmin, V. Sadovnichy, M. Sokolov, O. Pikin, and A. Amiraliev, "An original device for in-traoperative detection of small indeterminate nodules," *Eur. J. Cardiothorac Surg.*, vol. 46, pp. 1027–1031, Dec. 2014.

[7] R. F. Solodova, V. V. Galatenko, E. R. Nakashidze, I. L. Andreytsev, A. V. Galatenko, D. K. Senchik, V. M. Staroverov, V. E. Podolskii, M. E. Sokolov, and V. A. Sadovnichy, "Instrumental tactile diagnostics in robot-assisted surgery," *Med. Devices (Auckl)*, vol. 9, pp. 377–382, Oct. 2016.

[8] M. Sokolov, R. Solodova, V. Galatenko, V. Staroverov, and E. Nakashidze, "Tactile diagnostics in robotic surgery," *Eur. J. Surg. Oncol.*, vol. 42(9), pp. 73–73, 2016.

[9] R. F. Solodova, V. V. Galatenko, E. R. Nakashidze, S. G. Shapovalyants, I. L. Andreytsev, M. E. Sokolov, and V. E. Podolskii, "Instrumental mechanoreceptoric palpation in gastrointestinal surgery," *Minim. Invasive Surg.*, vol. 2017, Dec. 2017.

[10] G. Kharaishvili, D. Simkova, K. Bouchalova, M. Gachechiladze, N. Narsia, and J. Bouchal, "The role of cancer-associated fibroblasts, solid stress and other microenvironmental factors in tumor progression and therapy resistance," *Cancer Cell Int.*, vol. 14, no. 1, Article 41, May 2014.

[11] R. F. Solodova, V. M. Staroverov, V. V. Galatenko, A. V. Galatenko, E. V. Solodov, A. P. Antonov, V. M. Budanov, M. E. Sokolov, and V. A. Sadovnichy, "Automated detection of heterogeneity in medical tactile images," *Stud. Health Technol. Inform.*, vol. 220, pp. 383–389, 2016.

[12] S. A. Nersisyan and V. M. Staroverov, "Gradient estimation for hexagonal grids and its application to classification of instrumentally registered tactile images," *WSEAS Tr. on Appl. and Theor. Mech.*, vol. 13, no. 13, pp. 123–129, 2018.

[13] V. M. Staroverov, V. V. Galatenko, T. V. Zykova, Y. I. Rakhmatulin, D. V. Rukhovich, and V. E. Podolskii, "Automated real-time correction of intraoperative medical tactile images: sensitivity adjustment and suppression of contact angle artifact," *Appl. Math. Sci.*, vol. 10, no. 57, pp. 2831–2842, 2016.

[14] C. Cortes and V. Vapnik, "Support-Vector Networks," *Mach. Learn.*, vol. 20, no. 3, pp. 273–297, Sept. 1995.

[15] T. Cover and P. Hart, "Nearest neighbor pattern classification," *IEEE Trans. on Inf. Th.*, vol. 13, no. 1, pp. 21–27, Jan. 1967.